Master of Science

Pde6b knockout 쥐에서 유리체강 내 및 망막하 주사를 통한 AAV 2, 5, 8형의 망막 형질 전달 비교 평가

Comparative Evaluation of AAV Serotypes 2, 5, and 8 for Retinal Transduction in Pde6b Knockout Rats: Insights from Intravitreal and Subretinal Injections

The Graduate School
of the University of Ulsan

Department of Medicine
Jiehoon Kwak

Comparative Evaluation of AAV Serotypes 2, 5, and 8 for Retinal Transduction in Pde6b Knockout Rats: Insights from Intravitreal and Subretinal Injections

Supervisor : Joo Yong Lee

A Dissertation

Submitted to
the Graduate School of the University of Ulsan
In partial Fulfillment of the Requirements
for the Degree of

Master of Science

by

Jiehoon Kwak

Department of Medicine
Ulsan, Korea
Feburary 2024

Comparative Evaluation of AAV Serotypes 2, 5, and 8 for Retinal Transduction in Pde6b Knockout Rats: Insights from Intravitreal and Subretinal Injections

This certifies that the dissertation of Jiehoon Kwak is approved.

Junyeop Lee
Committee Chair Dr.

Joo Yong Lee
Committee Member Dr.

Yoon Jeon Kim
Committee Member Dr.

Department of Medicine
Ulsan, Korea
Feburary 2024

Abstract

Introduction : To assess the transduction efficiency of AAV serotypes 2, 5, and 8 in the outer retina of Pde6b knockout rats and Sprague-Dawley rats, via route of intravitreal and subretinal injection techniques.
Method : GFP-tagged AAV serotypes 2, 5, and 8 were administered via intravitreal or subretinal injection in Pde6b knockout rats at 3 weeks of age. Weekly in vivo fluorescence retinal imaging was conducted to monitor gene transfection distribution and assess the safety profile. After 6 weeks post-injection, the rats were euthanized, and the efficiency of retinal transduction was evaluated by analyzing fluorescence intensity of confocal microscope images following immunostaining. Additionally, the same methodology was applied to 7-week-old Sprague-Dawley rats, and they were monitored at 4, 8, 12, and 16 weeks for comparative analysis.
Result : In Pde6b knockout rats that underwent subretinal injection, all three AAV serotypes successfully transduced photoreceptors and RPE cells in a similar pattern. In contrast, upon intravitreal injection, both AAV5 and AAV8 demonstrated a lack of transduction in both the inner and outer retina. Only AAV2 exhibited retinal tropism, although its effectiveness in the outer retina was limited. In Pde6b knockout rats, quantitative fluorescence analysis revealed that AAV5 exhibited a stronger fluorescence intensity in vivo and higher transduction in immunostaining compared to AAV2 and AAV8 after subretinal injection. Similarly, while only AAV2 successfully transduced the inner retina after intravitreal injection, all three AAV serotypes transfected the outer retina following subretinal injection in unaffected rats. Furthermore, except for procedure-related media opacity, no adverse side effects were observed.
Conclusion : The subretinal injection of GFP-tagged AAV5 demonstrated higher transduction and retinal tropism than AAV2 and 8 in Pde6b knockout rats, suggesting its potential utilization in future clinical trials.

Keywords : Viral Tropsim, Pde6b protein, Om45-GFP protein, Photoreceptor cells

Index

Figures

Introduction

Merging at the forefront of therapeutic innovation, gene therapy has positioned itself as a compelling solution for previously incurable retinal diseases, such as inherited retinal disease (IRD) and age-related macular degeneration (AMD). The groundwork for this development was laid with the success of voretigene neparvovec-rzyl in the management of Leber's Congenital Amaurosis in 2017[1]. This breakthrough has paved the way for adeno-associated virus (AAV)-based gene therapies to become a primary focus in ophthalmological research, as indicated by the considerable number of ongoing clinical trials in this area[2].

The advantages of recombinant AAV as a gene therapy vector are multifaceted, primarily characterized by its safety and efficiency. AAV is inherently non-pathogenic and elicits a minimal immune-mediated inflammatory response. Importantly, it exists as episomes and does not integrate with the host genome, significantly reducing the risks of insertional mutagenesis and potential long-term adverse effects[3,4]. Furthermore, AAV facilitates long-term gene expression in post-mitotic retinal cells following transduction and exhibits considerable tropism for various retinal cell types, dependent on its serotypes. Efforts are currently underway to augment transduction efficiency by modifying promoters, enhancers, and through the development of capsid-recombinant AAVs.

The transduction efficiency of the AAV vector is known to vary in accordance with serotypes and administration routes. Several AAV serotypes, including 1, 2, 5, 7, 8, and 9, have demonstrated effective transduction of photoreceptors when administered through subretinal injections in rodent[5–7]. However, outer retinal transduction is relatively limited following intravitreal injections due to the presence of the internal limiting membrane as a barrier[8]. Notwithstanding, AAV2 and AAV8 have demonstrated their ability to transduce retinal ganglion cells, and engineered AAV2.7m8 has shown potential in transducing retinal photoreceptors, thereby overcoming the limitation of the internal limiting membrane[9]. As of 2022, over 46 clinical trials for retinal gene therapy

based on AAV are in progress, with the majority employing AAV-2 (57.4%) and AAV-8 (25.5%) subtypes. The route of administration is selected based on the target retinal layer and the retinal tropism of the AAV subtypes, with 52.6% of trials utilizing subretinal injection and 35.1% employing intravitreal injection[2].

Pde6b is beta subunit of PDE6, encoded by Pde6b gene, and plays an adjunctive role in hydrolysis of cGMP in phototransduction cascade cGMP-phosphodiesterase(PDE)[10,11]. Mutation in Pde6b gene lead to decrease in the activity of cGMP-PDE, which cause accumulation of cGMP in rod photoreceptors. Among autosomal recessive RP(retinitis pigmentosa) patients, Pde6b mutations accounts for 5-8% but lacks definite treatment, requiring the development of gene therapy[12–14]. While the retinal tropism of AAV in rats has been extensively studied, there remains a dearth of consensus concerning optimal intraocular gene transfer in mutant rats. This study endeavors to address this knowledge gap by investigating the tropism of AAV serotype 2, 5, and 8 via subretinal and intravitreal injections in Pde6b knockout rats and unaffected rats. The findings of this investigation are intended to provide critical insights that will contribute to the design and implementation of future clinical trials.

Methods

AAV Preparation

Animal Care and Preparation

In the experiments, a total of twelve 7-week-old Sprague-Dawley rats and sixteen 3-week-old Pde6b-knockout rats, which were produced by CRISPR-Cpf1 in our previous publishments[15], were utilized. The rats were assigned into two respective groups and subsequently received intravitreal and subretinal injections of AAV2, 5, and 8, which were tagged with green

fluorescent protein (GFP). To assess the retinas of the rats, retinal photography, optical coherence tomography, and in vivo fluorescence retinal imaging were performed on a weekly basis. The fluorescence levels in Sprague-Dawley rats were monitored for a duration of up to 8 weeks post-injection, while in Pde6b-knockout rats, the monitoring period lasted for 6 weeks post-injection. At 4 and 8 weeks after injection, the Sprague-Dawley rats were subgrouped and subsequently sacrificed for retinal wholemount and immunostaining procedures. Similarly, the same procedures were carried out on the Pde6b-knockout rats 6 weeks after injection. All live rat experiments were approved by the Institutional Animal Care and Use Committee of Asan Medical Center (Seoul, Korea). All animals were treated, maintained, and euthanized in accordance with the policies specified in the ARVO statement for the Use of Animals in Ophthalmic and Vision Research and the guidelines approved by national and local institutions

Intravitreal and subretinal injection protocol

The Sprague-Dawley rats, aged P49, were divided into two groups for intravitreal and subretinal injections (N=12). Each group consisted of six individuals and received one of three treatments: AAV2-GFP (N=4), AAV5-GFP (N=4), or AAV8-GFP (N=4). Pde6b-knockout rats, aged P21, were similarly segregated into two groups: intravitreal injection group (N=12) and subretinal injection group (N=12). Each group received either AAV2-GFP (N=4), AAV5-GFP (N=4), or AAV8-GFP (N=4).

The rats were anesthetized through an intraperitoneal injection of a combination of zolazepam and tiletamine at a dose of 12.5 mg/kg. The intravitreal injections were administered using a 33-G Hamilton syringe (Hamilton, Bonaduz, Switzerland), and the procedure was guided by an operating microscope (Zeiss, Oberkochen, Germany). The pupil dilation was achieved using Mydrin-P, consisting of tropicamide 5 mg/mL and phenylephrine 5 mg/mL (Santen Pharmaceuticals).

For intravitreal injections, a sclerotomy was carefully performed

approximately 1 mm posterior to the limbus using a 33-G Hamilton syringe. This was done with due care to avoid causing any damage to the lens. An amount of 5 μL AAV2,5,8-GFP (5.02 × 10^10 IPs) was administered intravitreally.

The subretinal injection required a temporal conjunctival periotomy, after which the subretinal injection was carried out using the same needle and the same dose of AAV2,5,8-GFP.

The accuracy of each injection was assessed via a fundus camera and in vivo fluorescence imaging as previously described. After imaging, the eyes were treated with Tarivid ointment (Ofloxacin 3mg/g; Santen Pharmaceuticals, Osaka, Japan) to prevent excessive dehydration during recovery.

In Vivo Imaging and Fluorescence measurement

In vivo retinal imaging and optical coherence tomography (OCT) were conducted utilizing Micron IV + OCT (Phoenix MICRON Image-Guided OCT2, Phoenix Laboratories, Pleasanton, CA, USA.) This imaging procedure was carried out on anesthetized rats, prepared by administering systemic anesthesia and inducing pupil dilation. The rats were sedated using 5% isoflurane and subsequently anesthetized via intraperitoneal injection of zolazepam and tiletamine (12.5 mg/kg), supplemented with xylazine (7.8 mg/kg). After the induction of anesthesia, Mydrin-P eye drops (consisting of tropicamide 5 mg/mL and phenylephrine 5 mg/mL; provided by Santen Pharmaceuticals, Osaka, Japan) were applied to each rat to stimulate mydriasis.

Upon anesthesia, the rat was then securely stationed on an adjustable base (SL20/M; Thorlabs, Newton, NJ, USA).This arrangement provided the flexibility to precisely manipulate the angles and positions for imaging, thus guaranteeing an extensive overview of the retina during the procedure. For capturing images of the targeted regions with precision, the rat's orientation was modified in four directions around the optic nerve to obtain

fluorescence images. The ability to return to the exact location for further analyses was ensured by using the distinctive vascular patterns as a reference, which stood out clearly against the fundus autofluorescence.

The assessment of GFP expression involved measuring GFP intensity across images using the FIJI software (National Institutes of Health, Bethesda, MD, USA). Two separate examiners (K.J.H and Y.J.M) were blinded to the images. The fluorescence distribution area of in vivo fundus photography was measured as the mean gray value after undergoing the following pre-processing steps: 1) splitting the RGB channel, 2) performing background subtraction, 3) applying Tsai moment-preserving thresholding, and 4) measuring the mean gray value corresponding to the region of interest[16]. For the fluorescence intensity of the retinal section, the pre-processed GFP+ channel was measured after the segmentation of the retinal layers. During the analysis of post-immunostaining confocal microscopy images, segmentation of the inner and outer nuclear layers was facilitated by the FIJI TUNEL cell counter plugin, if feasible[17]. If the segmentation did not perform as expected, manual ROI selection was performed by two separate examiners three times each, and the median value was chosen.

Sample Preparation and Immunostaining Protocol

Eye frozen sections were prepared to investigate the expression of target proteins using immunostaining. Tissue sections obtained from the eyes were fixed in 1XPBST for 15 minutes, repeated three times, to ensure proper fixation. For staining, a combination of green fluorescent protein (GFP) and 4',6-diamidino-2-phenylindole (DAPI) was used.

To commence the immunostaining protocol, the fixed sections underwent a series of washing steps with 1XPBST for 15 minutes, repeated three times, to remove any residual fixative and optimize antibody penetration. Blocking was then performed at room temperature for 1 hour to minimize non-specific binding and enhance the specificity of the subsequent antibody labeling. The sections were subsequently incubated with the primary antibody (1Ab solution) overnight at 4°C to enable specific binding

to the target proteins of interest.

Following the primary antibody incubation, the sections underwent further washing steps with 1XPBST for 15 minutes, repeated three times, to remove unbound primary antibodies. To visualize the primary antibody binding, the sections were then incubated with the appropriate secondary antibody (2Ab solution) for 1 hour and 30 minutes at 4°C. Subsequent to the secondary antibody incubation, additional washing steps with 1XPBST were performed to eliminate any unbound secondary antibodies. To visualize the nuclei, DAPI staining was conducted for 1 minute, allowing for precise localization of cellular structures. Finally, the sections were mounted, preserving the immunostaining pattern, and facilitating subsequent microscopic examination and data analysis.

Result

In this study, Pde6b KO rats were injected via intravitreal or subretinal route with AAV-GFP at postnatal day 21 (P21). Subsequent evaluations were performed weekly (on days P21, P28, P35, P42, P49, P54, and P63) using in vivo fluorescence imaging and slit-lamp examination. The rats were euthanized on P63 for subsequent immunostaining. Within the subretinal injection group, all three serotypes successfully transfected the photoreceptor (PR) and retinal pigment epithelium (RPE), as evidenced by the comparison of fluorescence intensities (Panel M and N of **Figure 1**). Interestingly, the fluorescence intensities of AAV5 were the highest and were not statistically different from AAV2, but statistically exceeded that of AAV8. Within the intravitreal injection cohort, AAV2 demonstrated minimal transduction of the inner nuclear layer, while AAV5 and AAV8 showed no evidence of fluorescently positive retinal cells at P63 (as depicted in left panel of **Figure 1)**. Notably, AAV2 transfected both the inner and outer retina, whereas AAV5 and AAV8 were unable to transduce the outer retinal layer.

In order to verify the retinal tropism of the AAV vectors used in the experiment, the same AAV-GFP were injected into Sprague-Dawley rats on P49, and they were subsequently examined in a similar manner on a weekly basis. These rats were euthanized on P57, P85, P113, and P141 for immunostaining. AAV2 and AAV5 showed pronounced retinal tropism, including in the PR and RPE, compared to AAV8, via subretinal injection. These findings were in accordance with those reported in previous publications[5,18–20]. Moreover, AAV2 demonstrated the highest inner retinal tropism via intravitreal injection (Left panel of **Figure 2**). As depicted in **Supplementary Figure 1**, AAV2 successfully transduced the inner retina, as evidenced by the presence of fluorescence-positive cells in perivascular retinal tissue in high magnification confocal images, which is located beneath inner limiting membrane.

Our study employed repeated in vivo fluorescence imaging and slit-lamp on a weekly basis in an attempt to evaluate the efficiency, distribution, and safety of retinal transfection using AAV-GFP. No AAV-associated adverse events, including inflammation, were observed with slit lamp in Pde6b knockout rats and controls, regardless of the injection route. Two cases of media opacities were reported after intravitreal injections in Sprague-Dawley rats **(Supplementary Figure 2)**. One case of mortality was recorded in a Pde6b knockout rat during the anesthesia procedure prior to subretinal injection. Furthermore, the fundus camera's 2D images hinder layer-by-layer analysis and observations hindered from vitreous clumps post-intravitreal injection, yet these limitations notwithstanding, we found a correlation between the overall results of the in vivo fluorescence imaging and those of the immunostaining images. In Pde6b knockout rats treated with subretinal injection, as shown in the upper right image of **Figure 3**, diffuse fluorescence centered on the subretinal bleb location was observed in all three serotypes at two weeks after injection. The fluorescence tends to increase over time, while AAV5 tends to reach its peak at week three and then plateau. The overall fluorescence distribution and density was found to be highest in the AAV5-GFP subretinal injection group during

observation period, and all AAV serotypes demonstrated similar levels of fluorescence intensity at P63. As demonstrated in the left image of **Figure 3**, the intravitreal injection of AAV2-GFP displayed the highest retinal tropism compared to other serotypes in Pde6b knockout rats, with fluorescence intensity tending to increase within six weeks post-injection. The fluorescence was particularly noticeable in the inner retinal layer, as inferred from the fluorescence in the peripapillary area, which includes the retinal ganglion cell layers and the perivascular area situated within the inner plexiform layer.

Furthermore, the Pde6b knockout rats enrolled in the study exhibited progressive retinal degeneration. Retinal thickness decreased during weekly OCT exams, and DAPI-stained retinal sections revealed an overall thinning of the retina in Pde6b knockout rats compared to the control group. As a consequence of progressive retinal atrophy, the outer nuclear layer (ONL) and inner nuclear layer (INL) became indistinguishable (**Supplementary Figure 3**). These findings are consistent with our previously published research, which demonstrated that Pde6b knockout rats experience ONL degeneration beginning at 3 weeks postnatal, and ONL thinning continues until 16 weeks postnatal[15]. Throughout the six weeks following the injection, no discernible intraocular complications, such as vitreous hemorrhage or retinal detachment, were observed.

Discussion

Two crucial components must be considered in the realm of retinal gene therapy. The first component is the AAV capsid, which governs retinal tropism and transduction efficiency. The second component is the internal limiting membrane, retinal interneurons and glial cells which acts as a mechanical barrier and presents significant obstacles for outer retinal accessibility[8,21,22]. With the utilization of engineered, recombinant AAVs, a variety of strategies have been developed to transduce photoreceptors and RPE via intravitreal injection. Such strategies may involve the modification

of promoters or enhancers, usage of exosome-associated AAV or the inclusion of enzymes designed to dismantle the ILM[19,20,23,24]. While these contributions have significantly advanced the field of gene therapy, the in vivo safety of such interventions in humans is yet to be thoroughly established. Conversely, the safety of naïve AAVs administered via subretinal injection is well-documented, a fact that underpins their widespread use in the majority of current clinical trials focused on retinal gene therapy[2,25].

Numerous AAV serotypes have been discovered, with AAV1, AAV2, AAV7, AAV8, and AAV9 identified as being capable of successfully transducing the retina following subretinal injections in mutation-naive rats[3]. Various recombinant AAV are being experimented: Han et al issued that AAV2/1, AAV2/2, AAV2/6, AAV2/8 and AAV2/9 all transfected outer retina successfully after subretinal injection, while AAV2/1 showing highest retinal tropism[5]. They also noted that AAV2/1 and AAV2/6 were able to transduce primarily inner retina via intravitreal injection. Similarly in mouse, AAV 2,8 and 9 successfully transduced retina after subretinal injection[26]. In non-human primate, wild type AAV5 showed efficient transduction of PR after subretinal injection[6(p5)]. A direct comparison of the efficiency of retinal transduction among wildtype AAV serotypes is currently lacking. Our study provides valuable insights to this. We found that AAV2 demonstrated efficient transduction specifically in the inner retina, whereas AAV5 and AAV8 exhibited poor transduction following intravitreal injection in unaffected rats. Interestingly, all three AAV serotypes successfully transfected the outer retina after subretinal injection, which is consistent with previous publications.

Aside from recent publications detailing the treatment of Pde6b-deficient rats using subretinal injection of AAV2/1 and AAV2/5[27], the retinal tropism of different AAV serotypes in genetically modified rats has been largely unexplored. In the present study, we have concluded that the subretinal injection of AAV5 yields comparable or superior retinal transduction compared to AAV2 and AAV8, both in terms of durability and efficiency.

This conclusion is supported by the extensive in vivo fluorescence imaging and the fluorescence intensity observed in retinal section images. Given that Pde6b is primarily located in the ONL, where it plays a crucial role in the breakdown of cGMP, a molecule involved in the signaling cascade of photoreceptor cells, the efficient transduction of the outer retina, including the ONL, by AAV5 holds promise for gene therapy targeting Pde6b-associated retinitis pigmentosa. Furthermore, AAV vector is known to possess a limited nucleotide storage capacity of up to 4.7kb. However, Allocca et al. proposed that recombinant AAV (rAAV) utilizing the AAV5 capsid could potentially increase this capacity up to 8.9kb[28]. Furthermore, the receptor binding mechanism of AAV5 is dependent on N-linked sialic acids, differing from AAV2, which depends on heparan sulfate proteoglycans[29,30]. This unique binding mechanism might allow AAV5 to be effective alternative in patients who have pre-existing immunity to AAV2. Since 2017, Coave Therapeutics is conducting Phase I/II clinical trials (NCT03328130) involving the subretinal injection of AAV2/5-hPde6b in patients with retinitis pigmentosa, utilizing the AAV5 capsid. We posit that AAV5 may serve as an alternative vector to AAV2 in the treatment of Pde6b mutation.

Additionally, our findings indicate disparities in tissue specificity among AAV2, AAV5, and AAV8 in both mutation-naive rats and genetically modified rats (**Figure 1** and **2**). We postulate that the retinal tropism observed in Pde6b knockout rats may not directly correlate to that in unaffected rats. Although less relevant, retinal tropism of AAV2,5,7 and 9 between normal mouse and diabetic mouse retina differs[31], and retinal tropism of AAV5, AAV9 and AAV6 variant differed in Crb1 mutant rat and control rat[32] . Although this current study does not provide direct evidence, it is plausible that the modified cellular response triggered by genetic mutations could alter the interaction between AAV and host tissues. Secondary to Pde6b mutation, reduction of functional enzyme may overregulate extracellular Pde6b receptor and abnormal trafficking of intracellular protein may change such interaction[33]. In Pde6b knockout rats, the progressive retinal degeneration depicted in **Supplementary Figure 3**

may disrupt the physiological and cellular barriers of the neuronal and glial tissues of the outer retina due to anatomical loosening while preserving ILM. Although we did not directly compare the fluorescence intensity between Pde6b knockout rats and unaffected rats, we observed consistent fluorescence intensity in the outer retina of Pde6b knockout rats following subretinal injection, which was not observed after intravitreal injection. This observation suggests that the dysmorphic outer retinal structures in the Pde6b knockout rats may facilitate efficient AAV distribution in the outer retina. Also, we carefully remark that AAV vectors tested in unaffected rats may not be effective in genetically modified models. Further investigations are warranted to validate this hypothesis and gain a deeper understanding of the implications of our findings.

Our study is subject to a few limitations. Firstly, we only injected adeno-associated viruses carrying the green fluorescent protein (AAV-GFP), not those storing therapeutic genes. Given that various intricate factors, such as tissue-specific promoters, immune responses, and transgenic effects, contribute to the success of retinal gene therapy, successful retinal transduction of AAV-GFP does not necessarily guarantee the success of gene therapy. However, we propose that AAV5 may serve as an alternative vector to AAV2. This suggestion could provide valuable insights for researchers developing AAVs, potentially saving both time and money, as preclinical trials on larger primates can be both costly and time-consuming. Second, we only evaluated the retinal sections of Pde6b knockout rats at P63. According to our previously published articles, the Pde6b knockout rats demonstrate extensive degeneration of the outer nuclear layer (ONL), and this degeneration continues to progress. Consequently, by 16 weeks, the ONL is no longer present. This could explain why the distribution and fluorescence of AAV5 plateaued three weeks post-injection (P42). The inherent characteristic of progressive retinal degeneration in Pde6b knockout rats may alter the retinal tropism of AAV vectors. Therefore, our study does not provide insights into gene transfection efficiency in rats with advanced retinal degeneration. Third, we did not perform electroretinogram or additional immunostaining other than

DAPI,e.g. Iba1 to quantify retinal inflammation[34], which might offer some clinical clues. Nevertheless, we concluded that our study design was sufficiently suitable for selecting AAV vectors for further gene therapy. Fourth, measuring the fluorescence intensity and distribution using FIJI can be error-prone since it does not capture the whole retina but only a portion of it. Additionally, the fact that degree of fluorescence of GFP does not directly correlate with retinal tropism and the success of gene therapy should be considered

Conclusion

In conclusion, our study provides important insights into the efficiency, distribution, and safety of retinal transfection using AAV2,5 and 8 in Pde6b knockout rats and control rats, despite certain limitations related to imaging modalities. We identified AAV2 as demonstrating high retinal tropism following intravitreal injection, while all AAV serotypes exhibited notable retinal tropism, including in the PR and RPE, following subretinal injection. Notably, the fluorescence intensity and distribution were higher for AAV5 as compared to AAV2 and AAV8. These findings underscore the potential utility of AAV5 as an alternative vector for retinal gene therapy. Additionally, no significant intraocular complications were observed, reinforcing the safety profile of these AAV vectors. Nevertheless, it is essential to consider the impact of factors such as tissue-specific promoters, immune response, and transgenic effects on the success of retinal gene therapy. Our results should inform future research and the development of gene therapy strategies associated with Pde6b-associated retinitis pigmentosa, potentially saving time and resources in preclinical trials. Further studies are needed to validate our findings and explore their implications in the context of advanced retinal degeneration and potential differences in tissue specificity and immune response among different AAV vectors.

Reference

1. Russell S, Bennett J, Wellman JA, et al. Efficacy and safety of voretigene neparvovec (AAV2-hRPE65v2) in patients with RPE65-mediated inherited retinal dystrophy: a randomised, controlled, open-label, phase 3 trial. *The Lancet*. 2017;390(10097):849-860. doi:10.1016/S0140-6736(17)31868-8

2. Cheng SY, Punzo C. Update on Viral Gene Therapy Clinical Trials for Retinal Diseases. *Hum Gene Ther*. 2022;33(17-18):865-878. doi:10.1089/hum.2022.159

3. Day TP, Byrne LC, Schaffer DV, Flannery JG. Advances in AAV Vector Development for Gene Therapy in the Retina. Ash JD, Grimm C, Hollyfield JG, Anderson RE, LaVail MM, Bowes Rickman C, eds. 2014;801:687-693. doi:10.1007/978-1-4614-3209-8_86

4. Vandenberghe LH, Wilson JM, Gao G. Tailoring the AAV vector capsid for gene therapy. *Gene Ther*. 2009;16(3):311-319. doi:10.1038/gt.2008.170

5. Han IC, Cheng JL, Burnight ER, et al. Retinal Tropism and Transduction of Adeno-Associated Virus Varies by Serotype and Route of Delivery (Intravitreal, Subretinal, or Suprachoroidal) in Rats. *Hum Gene Ther*. 2020;31(23-24):1288-1299. doi:10.1089/hum.2020.043

6. Lotery AJ, Yang GS, Mullins RF, et al. Adeno-associated virus type 5: transduction efficiency and cell-type specificity in the primate retina. *Hum Gene Ther*. 2003;14(17):1663-1671. doi:10.1089/104303403322542301

7. Pang J jing, Lauramore A, Deng W tao, et al. Comparative analysis of in vivo and in vitro AAV vector transduction in the neonatal mouse retina: Effects of serotype and site of administration. *Vision Res*. 2008;48(3):377-385. doi:10.1016/j.visres.2007.08.009

8. Dalkara D, Kolstad KD, Caporale N, et al. Inner Limiting Membrane Barriers to AAV-mediated Retinal Transduction From the Vitreous. *Mol Ther*. 2009;17(12):2096-2102. doi:10.1038/mt.2009.181

9. Dalkara D, Byrne LC, Klimczak RR, et al. In Vivo–Directed Evolution of a New Adeno-Associated Virus for Therapeutic Outer Retinal Gene Delivery from the Vitreous. *Sci Transl Med*. 2013;5(189):189ra76-189ra76. doi:10.1126/scitranslmed.3005708

10. Khramtsov N v., Feshchenko E a., Suslova V a., et al. The human rod photoreceptor cGMP phosphodiesterase β-subunit. *FEBS Lett*. 1993;327(3):275-278. doi:10.1016/0014-5793(93)81003-I

11. Cote RH. Characteristics of Photoreceptor PDE (PDE6): similarities and differences to PDE5. *Int J Impot Res*. 2004;16(1):S28-S33. doi:10.1038/sj.ijir.3901212

12. Oishi M, Oishi A, Gotoh N, et al. Comprehensive Molecular Diagnosis of a Large Cohort of Japanese Retinitis Pigmentosa and Usher Syndrome Patients by Next-Generation Sequencing. *Invest Ophthalmol Vis Sci*. 2014;55(11):7369-7375. doi:10.1167/iovs.14-15458

13. Kim MS, Joo K, Seong MW, et al. Genetic Mutation Profiles in Korean Patients with Inherited Retinal Diseases. *J Korean Med Sci*. 2019;34(21). doi:10.3346/jkms.2019.34.e161

14. Kim YN, Song JS, Oh SH, et al. Clinical characteristics and disease progression of retinitis pigmentosa associated with PDE6B mutations in Korean patients. *Sci Rep*. 2020;10(1):19540. doi:10.1038/s41598-020-75902-z

15. Yeo JH, Jung BK, Lee H, et al. Development of a *Pde6b* Gene Knockout Rat Model for Studies of Degenerative Retinal Diseases. *Investig Opthalmology Vis Sci*. 2019;60(5):1519. doi:10.1167/iovs.18-25556

16. Maidana DE, Notomi S, Ueta T, et al. ThicknessTool: automated ImageJ retinal layer thickness and profile in digital images. *Sci Rep*. 2020;10(1):18459. doi:10.1038/s41598-020-75501-y

17. Maidana DE, Tsoka P, Tian B, et al. A Novel ImageJ Macro for Automated Cell Death Quantitation in the Retina. *Invest Ophthalmol Vis Sci*. 2015;56(11):6701-6708. doi:10.1167/iovs.15-17599

18. Wiley LA, Burnight ER, Kaalberg EE, et al. Assessment of Adeno-Associated Virus Serotype Tropism in Human Retinal Explants. *Hum Gene Ther*. 2018;29(4):424-436. doi:10.1089/hum.2017.179

19. Dias MS, Araujo VG, Vasconcelos T, et al. Retina transduction by rAAV2 after intravitreal injection: comparison between mouse and rat. *Gene Ther*. 2019;26(12):479-490. doi:10.1038/s41434-019-0100-9

20. Issa PC, Silva SRD, Lipinski DM, et al. Assessment of Tropism and Effectiveness of New Primate-Derived Hybrid Recombinant AAV Serotypes in the Mouse and Primate Retina. *PLOS ONE*. 2013;8(4):e60361. doi:10.1371/journal.pone.0060361

21. Fischer MD, Huber G, Beck SC, et al. Noninvasive, In Vivo Assessment of Mouse Retinal Structure Using Optical Coherence Tomography. *PLOS ONE*. 2009;4(10):e7507. doi:10.1371/journal.pone.0007507

22. Snodderly DM, Weinhaus RS, Choi JC. Neural-vascular relationships in central retina of macaque monkeys (Macaca fascicularis). *J Neurosci*. 1992;12(4):1169-1193. doi:10.1523/JNEUROSCI.12-04-01169.1992

23. Wassmer SJ, Carvalho LS, György B, Vandenberghe LH, Maguire CA. Exosome-associated AAV2 vector mediates robust gene delivery into the murine retina upon intravitreal injection. *Sci Rep*. 2017;7(1):45329. doi:10.1038/srep45329

24. Weber M, Rabinowitz J, Provost N, et al. Recombinant adeno-associated virus serotype 4 mediates unique and exclusive long-term transduction of retinal pigmented epithelium in rat, dog, and nonhuman primate after subretinal delivery. *Mol Ther*. 2003;7(6):774-781. doi:10.1016/S1525-0016(03)00098-4

25. Sengillo JD, Justus S, Tsai YT, Cabral T, Tsang SH. Gene and cell-based therapies for inherited retinal disorders: An update. *Am J Med Genet C Semin Med Genet*. 2016;172(4):349-366. doi:10.1002/ajmg.c.31534

26. Petrs-Silva H, Dinculescu A, Li Q, et al. High-efficiency Transduction of the Mouse Retina by Tyrosine-mutant AAV Serotype Vectors. *Mol Ther*. 2009;17(3):463-471. doi:10.1038/mt.2008.269

27. Han IC, Wiley LA, Ochoa D, et al. Characterization of a novel Pde6b-deficient rat model of retinal degeneration and treatment with adeno-associated virus (AAV) gene therapy. *Gene Ther*. 2023;30(3-4):362-368. doi:10.1038/s41434-022-00365-y

28. Allocca M, Doria M, Petrillo M, et al. Serotype-dependent packaging of large genes in adeno-associated viral vectors results in effective gene delivery in mice. *J Clin Invest*. 2008;118(5):1955-1964. doi:10.1172/JCI34316

29. Akache B, Grimm D, Pandey K, Yant SR, Xu H, Kay MA. The 37/67-Kilodalton Laminin Receptor Is a Receptor for Adeno-Associated Virus Serotypes 8, 2, 3, and 9. *J Virol*. 2006;80(19):9831-9836. doi:10.1128/jvi.00878-06

30. Wu Z, Miller E, Agbandje-McKenna M, Samulski RJ. α2,3 and α2,6 N-Linked Sialic Acids Facilitate Efficient Binding and Transduction by Adeno-Associated Virus Types 1 and 6. *J Virol*. 2006;80(18):9093-9103. doi:10.1128/jvi.00895-06

31. Lee SH, Yang JY, Madrakhimov S, Park HY, Park K, Park TK. Adeno-Associated Viral Vector 2 and 9 Transduction Is Enhanced in Streptozotocin-Induced Diabetic Mouse Retina. *Mol Ther - Methods Clin Dev*. 2019;13:55-66. doi:10.1016/j.omtm.2018.11.008

32. Boon N, Alves CH, Mulder AA, et al. Defining Phenotype, Tropism, and Retinal Gene

Therapy Using Adeno-Associated Viral Vectors (AAVs) in New-Born Brown Norway Rats with a Spontaneous Mutation in Crb1. *Int J Mol Sci*. 2021;22(7):3563. doi:10.3390/ijms22073563

33. Gopalakrishna KN, Boyd K, Artemyev NO. Mechanisms of mutant PDE6 proteins underlying retinal diseases. *Cell Signal*. 2017;37:74-80. doi:10.1016/j.cellsig.2017.06.002

34. Wiley LA, Boyce TM, Meyering EE, et al. The Degree of Adeno-Associated Virus-Induced Retinal Inflammation Varies Based on Serotype and Route of Delivery: Intravitreal, Subretinal, or Suprachoroidal. *Hum Gene Ther*. 2023;34(11-12):530-539. doi:10.1089/hum.2022.222

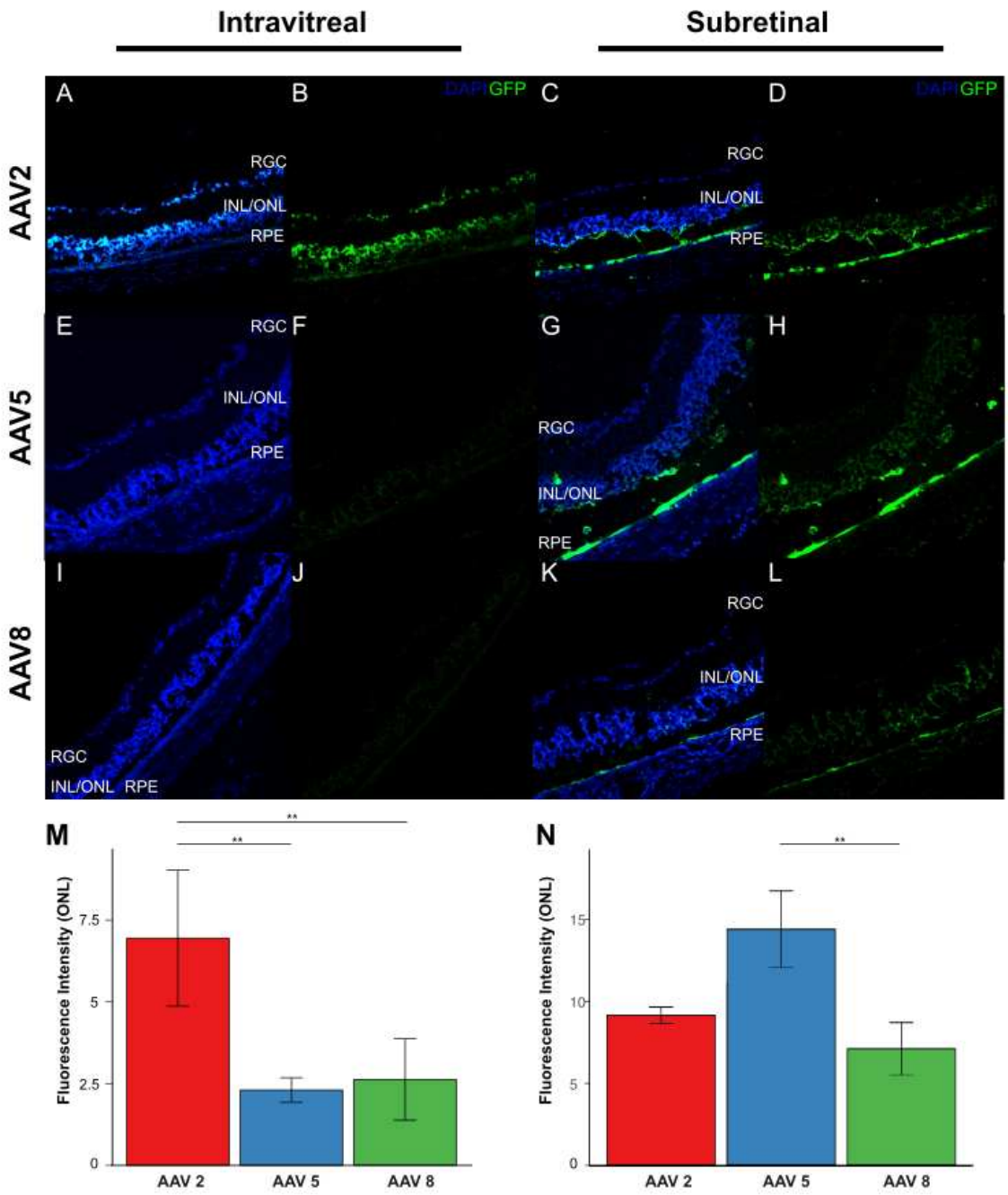

Figure 1. Immunohistochemical Staining of Pde6b Knockout Rats Following Intravitreal and Subretinal Injection, representing highest retinal transduction of AAV5 after subretinal injection. Panels (A, E, I) depict DAPI and GFP merged retinal sections following intravitreal injection, with each row representing a different AAV serotype. **Panels (B, F, J)** show corresponding GFP stained retinal sections. AAV2 successfully transfected both the inner and outer retina, with fluorescence intensity significantly higher than that of

AAV6 and AAV8 **(M)**. **Panels (C, G, K)** similarly represent merged retinal sections following subretinal injection. **Panels (D, H, L)** illustrate GFP-stained retinal sections. AAV2, 5, and 8 successfully transfected all retinal layers, with AAV5 exhibiting the highest fluorescence intensity in the outer nuclear layer and photoreceptor layer **(N)**.

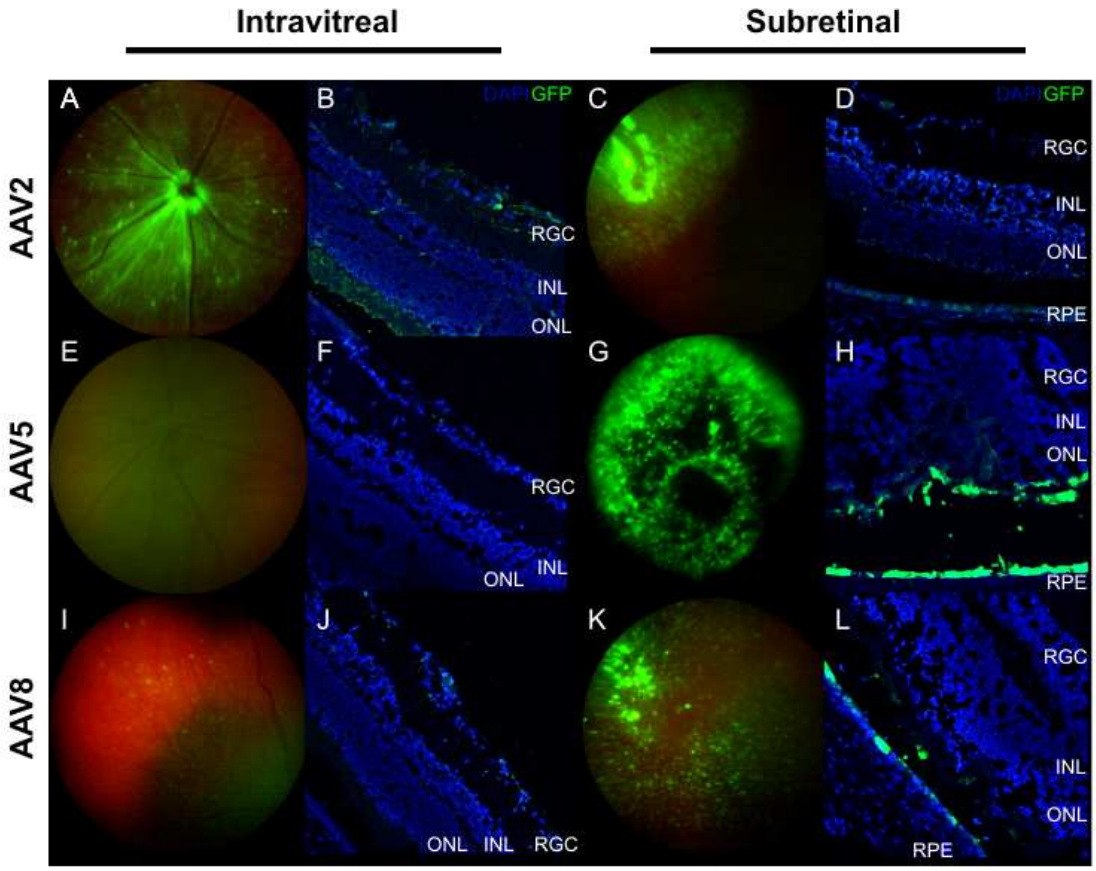

Figure 2. Retinal Tropism Following Intravitreal or Subretinal Injection of eGFP-AAV2, 5, and 8 in Sprague-Dawley Rats. Intravitreal injection groups were evaluated at 8 weeks post-injection, while subretinal injection groups were evaluated at 4 weeks post-injection. **Panels (A, E, I)** depict in vivo fluorescence fundus images taken 8 weeks after intravitreal injection, with AAV2 **(A)** demonstrating the highest fluorescence intensity. **Panels (B, F, J)** represent immunohistochemistry (IHC) with x200 magnification corresponding to the fundus images. AAV2 **(B)** successfully transduced retinal ganglion cells (RGCs), the inner nuclear layer (INL), and the outer nuclear layer (ONL), while fluorescence was minimal with AAV5 **(F)** and AAV8 **(J)**. **Panels (C, G, K)** depict fundus images taken 4 weeks after subretinal injection. All AAV serotypes exhibited stronger fluorescence intensity compared to intravitreal injection, with AAV5 **(G)** showing the highest fluorescence intensity and distribution. **Panels (D, H, L)** represent

IHC, with all AAV serotypes successfully transducing all retinal layers. AAV5 (**H)** demonstrated strong fluorescence in the photoreceptor layer and retinal pigment epithelium (RPE).

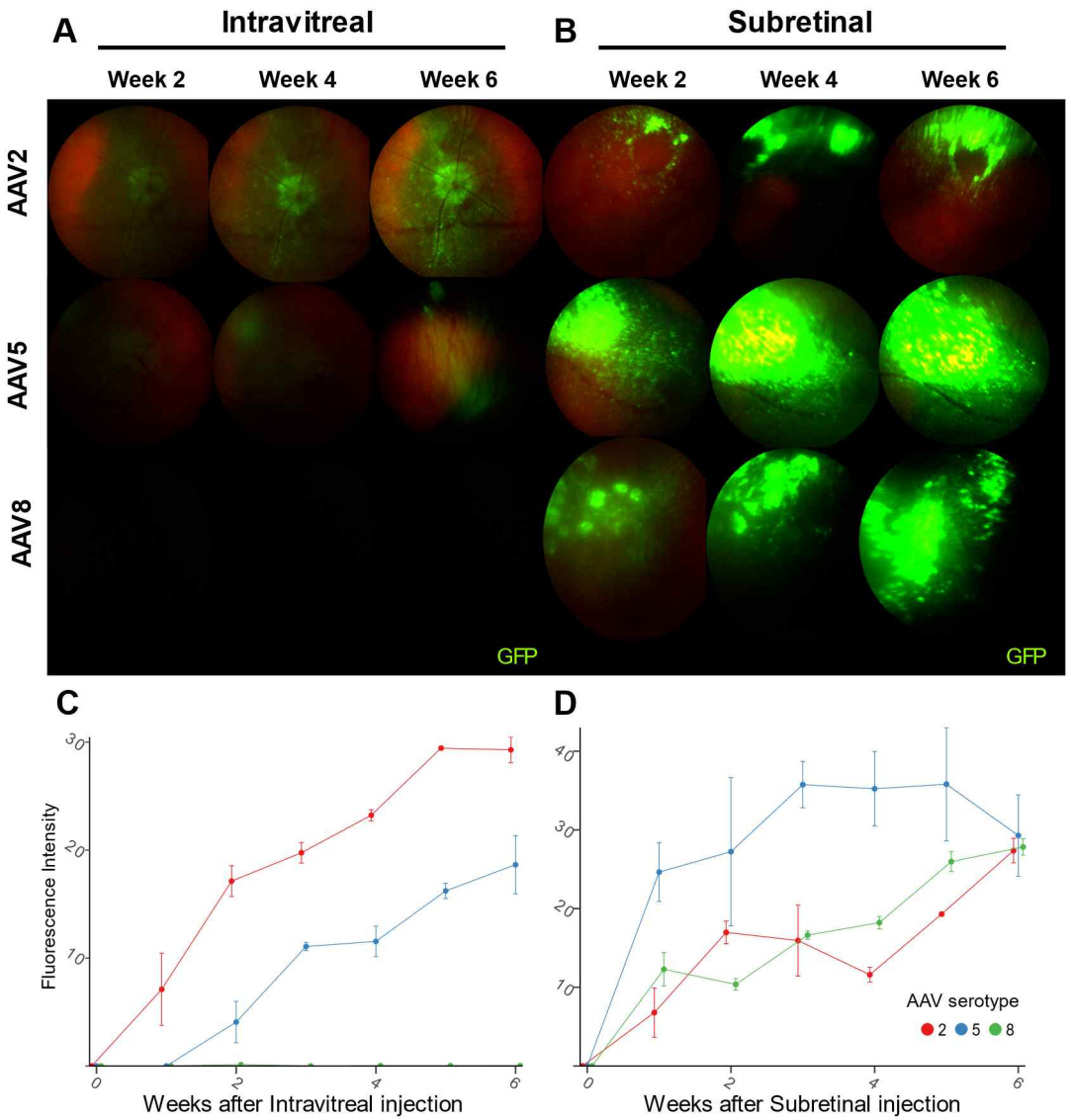

Figure 3. Retinal Tropism in Pde6b Knockout Rats Following Intravitreal and Subretinal Injection. Panels (A, B) depict in vivo fluorescence fundus images, with rows representing AAV serotypes and columns representing weeks post eGFP-AAV injection. **Panel (C)** presents total fluorescence intensity after intravitreal injection, while **panel (D)** represents total fluorescence intensity following subretinal injection. rAAV2 demonstrates the highest retinal transduction distribution via intravitreal injection (refer to **panel A**, top row; and **panel C**). AAV serotypes 2, 5, and 8 successfully transduced the retina, whereas AAV5 exhibited the highest fluorescence

intensity over time (refer to **panel D**) and the broadest distribution (refer to **panel B**).

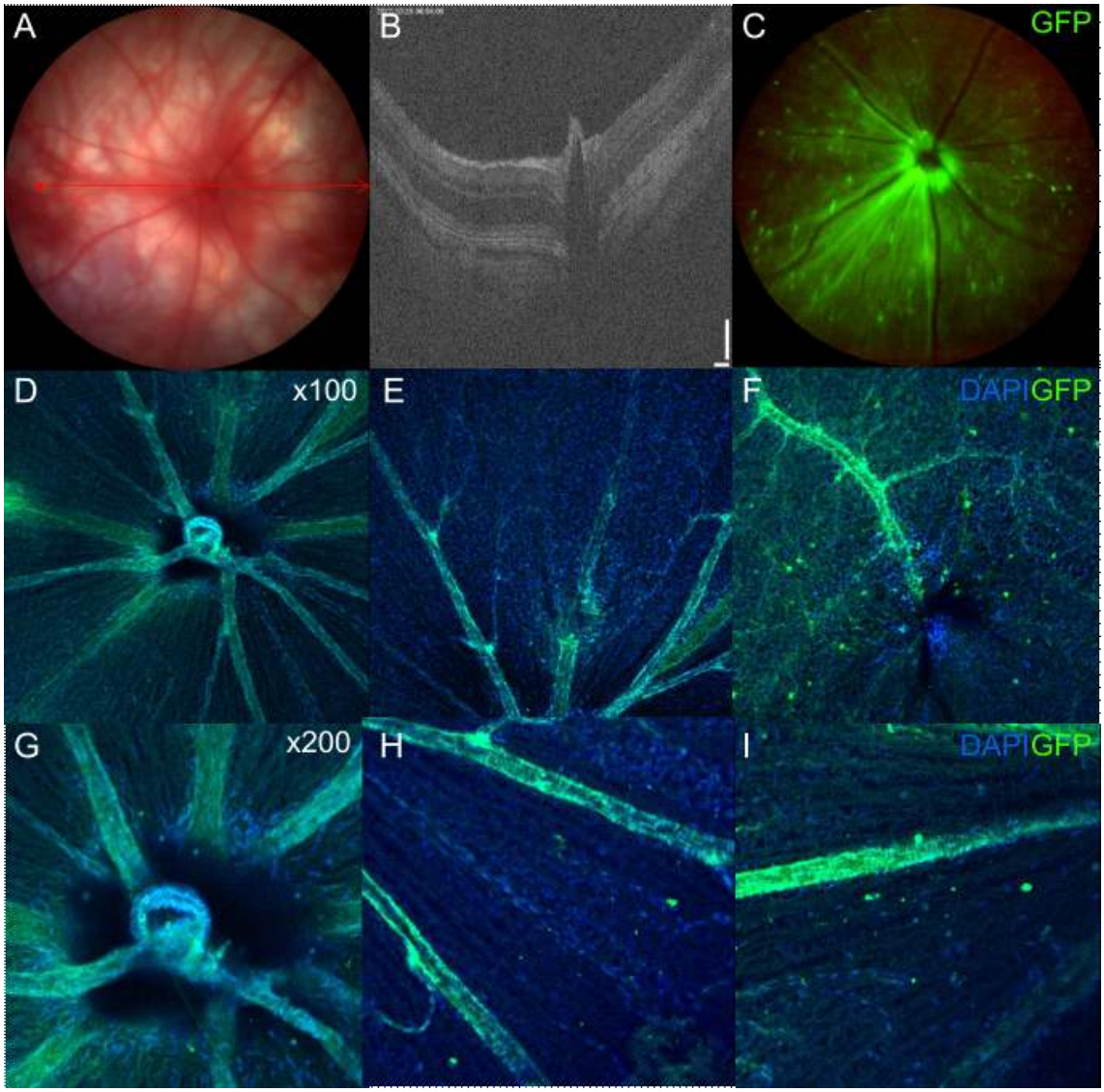

Supplementary Figure 1. Retinal Tropism in Sprague-Dawley Rats Injected Intravitreally with AAV2-eGFP. (A) Fundus Photography; **(B)** Optical Coherence Tomography (OCT) of the area corresponding to the red arrow in panel A; **(C)** In Vivo Fluorescence Fundus Photography displaying green fluorescing cells, indicative of GFP transduction; **(D, E, F)** Immunostaining with DAPI and GFP after whole mount preparation, depicted at 100x magnification at 8 weeks post-injection. These images highlight perivascular enhancement and GFP(+) retinal nuclei; **(G, H, I)** Additional Immunostaining images provided at 200x magnification.

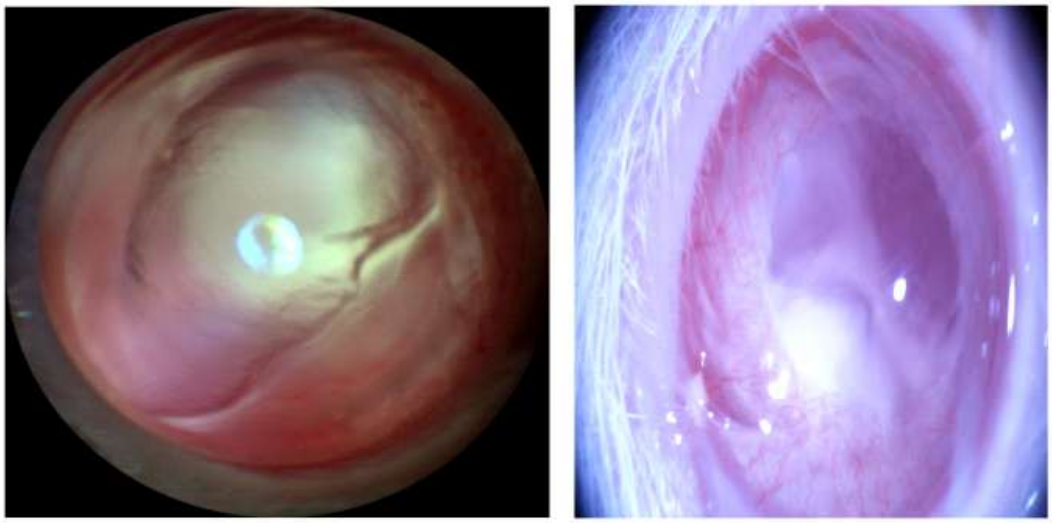

Supplementary Figure 2. Two cases of corneal opacities after intravitreal injection of AAV5-GFP in Sprauge-Dawley rats.

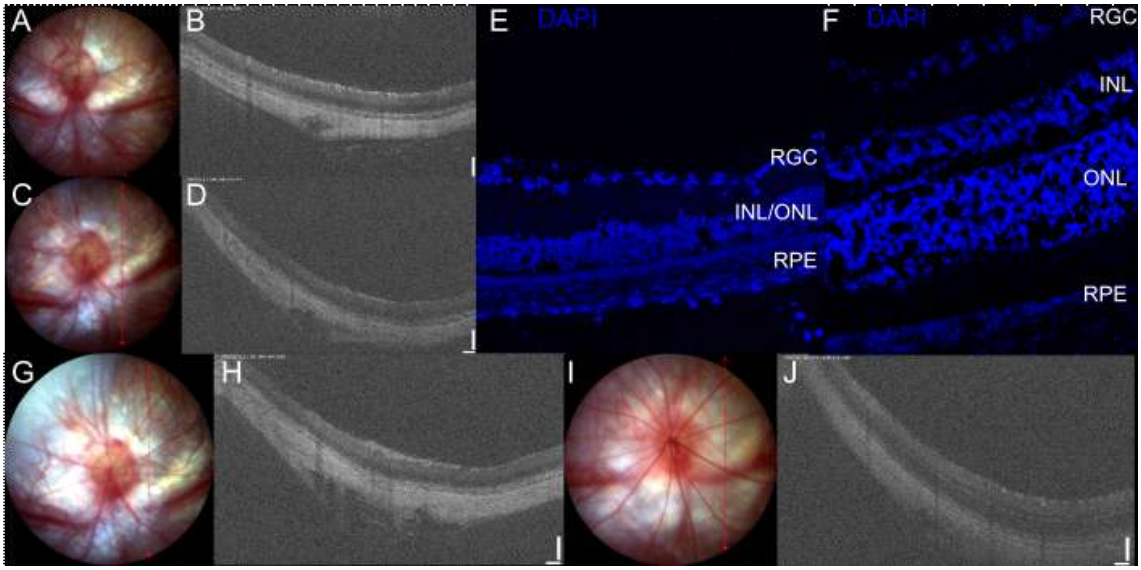

Supplementary Figure 3. Anatomical Differences in the Retina Between Pde6b Knockout Rats and Sprague-Dawley Rats. Panels (A, C, G, I) depict fundus photography of Pde6b knockout rats at ages P21, P42, P63, and Sprague-Dawley rats at P63, respectively. These images highlight progressive retinal depigmentation and arteriolar attenuation when compared to the control **(I)**. **Panels (B, D, H, J)** correspond to optical coherence tomography of the same rats as in **(A, C, G, I)**, respectively, indicating a progressive decrease in retinal thickness. The scale bar represents 100μm. **Panel (E)** presents a DAPI-stained retinal section with x200 magnification from a P63 Pde6b knockout rat, demonstrating atrophy of the outer retinal layer, which obscures the distinction between the inner nuclear layer(INL) and the outer nuclear layer(ONL). Panel (F) shows a DAPI-stained retinal section from a P63 Sprague-Dawley rat, exhibiting a clearly distinguishable retinal structure.

국문요약

목적: Pde6b 녹아웃 쥐와 Sprague-Dawley 쥐의 외망막에서 AAV 2, 5, 8형의 전달 효율을 비교 및 평가하고자 하였다.

방법: GFP 표지 AAV 2, 5, 8형을 생후 3주 된 Pde6b 녹아웃 쥐에 유리체강 내 및 망막하 주사로 투약하였다. 매주 생체 형광 망막 영상을 촬영하여 유전자 전달 분포를 모니터링하고 안전성을 평가하였다. 주사 6주 후에 쥐를 안락사시키고 형광 현미경 이미지의 형광 강도를 면역 염색 후 분석하여 망막 전달 효율을 평가하였다. 또한 동일한 방법을 7주 된 Sprague-Dawley 쥐에게 적용하고 4주, 8주, 12주, 16주에 비교 분석을 위해 면역 염색을 시행하였다.

결과: 망막하 주사를 시행한 Pde6b 녹아웃 쥐에서 세 가지 AAV 형 모두 유사한 패턴으로 광수용체와 망막색소상피세포에 성공적으로 전달되었다. 반면 유리체강내 주사를 시행한 군에서는 AAV5와 AAV8 모두 내망막과 외망막 모두에서 전달이 부족한 것으로 나타났다. AAV2만이 망막 친화성을 보였지만 외망막에서의 효과는 제한적이었다. Pde6b 녹아웃 쥐에서 정량적 형광 분석 결과, AAV5는 망막하 주사 후 AAV2와 AAV8에 비해 더 강한 형광 강도를 보였고 면역 염색에서 더 높은 전달 효율을 보였다. 마찬가지로 Sprague-Dawley 쥐에서는 유리체강 내 주사 후에는 AAV2만 내망막에 성공적으로 전달되었지만, 망막하 주사 후 세 가지 AAV 형 모두 외망막에 전달되었다. 또한 주사 관련 매체 혼탁을 제외하고는 AAV 관련 면역 부작용은 관찰되지 않았다.

결론: GFP 표지 AAV5의 망막하 주사는 Pde6b 녹아웃 쥐에서 AAV2와 8보다 높은 망막 전달 효율과 친화성을 보였으며, 향후 임상 시험에 활용될 가능성을 시사한다.